ARTICLE

OBC
www.rsc.org/obc

Evodiamine functions as an agonist for the vanilloid receptor TRPV1

Larry V. Pearce,[a] Pavel A. Petukhov,[b] Tamas Szabo,[a] Noemi Kedei,[a] Fero Bizik,[b] Alan P. Kozikowski[b] and Peter M. Blumberg*[a]

[a] *Laboratory of Cellular Carcinogenesis and Tumor Promotion, Center for Cancer Research, National Cancer Institute, Building 37, Room 4048, 37 Convent Drive MSC 4255, Bethesda, MD 20892-4255, USA. E-mail: blumberp@dc37a.nci.nih.gov; Fax: +301-496-8709; Tel: +301-496-3189*

[b] *Department of Medicinal Chemistry and Pharmacognosy, University of Illinois at Chicago, IL, 60612-2730, USA*

Received 26th March 2004, Accepted 29th June 2004
First published as an Advance Article on the web 27th July 2004

Evodiamine, a quinozole alkaloid constituent of *Evodia rutaecarpa*, has been reported previously to induce several responses comparable to capsaicin in animal systems. Here, we characterize evodiamine as an agonist for rat TRPV1 expressed heterologously in CHO cells. Evodiamine bound to rat TRPV1 with a K_i of 5.95 ± 0.87 μM, as measured by inhibition of [^{3}H] RTX binding (capsaicin, K_i = 1.8 ± 0.3 μM). Evodiamine was a full agonist for induction of $^{45}Ca^{2+}$ uptake, with an EC_{50} of 856 ± 43 nM (capsaicin, EC_{50} = 45 ± 4 nM) and was competitively antagonized by capsazepine, as revealed by a Schild plot. The pattern of cellular response, as determined by calcium imaging, was similar to that with capsaicin and yielded an EC_{50} of 1.03 ± 0.21 μM. Molecular modeling suggested a consistent pattern of overlap between evodiamine and TRPV1 agonists. We conclude that evodiamine represents a novel class of agonists for rat TRPV1, albeit 3–19-fold less potent than capsaicin, and thus represents a new potential class of lead molecules for drug development.

Introduction

The vanilloid receptor subtype 1 (TRPV1) is a cation channel on C-fiber sensory neurons that is activated by protons, heat, and a variety of pungent chemicals, such as capsaicin (CAP) and resiniferatoxin (RTX).[1] The activation of TRPV1 by vanilloid agonists results in calcium influx and, to a lesser extent, the release of calcium stores from the endoplasmic reticulum.[2] The rapid influx of calcium is followed by a long refractory state or desensitization of the receptor, rendering it less sensitive to subsequent applications of painful stimuli. Because of the important physiological roles of C-fiber neurons, TRPV1 has attracted much attention as a therapeutic target for the treatment of chronic pain, as well as other conditions such as bladder hyperreflexia.

Although capsaicin represents the best characterized agonist for TRPV1, a variety of other natural products and endogenous compounds have since been identified which also function as agonists for the receptor.[3] Among these, resiniferatoxin is orders of magnitude more potent than capsaicin, and anandamide and arachidonyl dopamide are putative endogenous regulators.

The dried fruits of *Evodia rutaecarpa* constitute the Chinese herbal medicine Wu-Zhu-Yu. Recently, evodiamine (Fig. 1), isolated from *E. rutaecarpa*, was described by Kobayashi and co-workers as a putative TRPV1 agonist.[4–6] They showed that evodiamine induced several biological responses in a similar fashion to capsaicin. These responses included contraction of isolated guinea pig bronchus, cardiotonic effects on isolated guinea pig atria, irritation in the mouse paw licking assay, and inhibition of acetic acid-induced writhing in the mouse. Evodiamine and capsaicin caused cross-tachyphylaxis in the guinea pig systems and the irritant action of evodiamine was inhibited by capsazepine, a capsaicin antagonist.

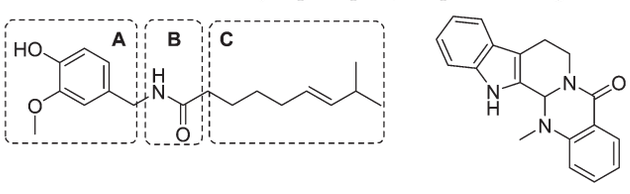

Capsaicin Evodiamine

Fig. 1 Chemical structure of capsaicin and evodiamine.

Because the structure of evodiamine shows little homology with capsaicin, it represents a potential novel structural lead for the development of TRPV1 ligands. In this report, we therefore examined evodiamine directly as a ligand for TRPV1. We conclude that it indeed functions as a TRPV1 agonist, albeit with a potency 3–19-fold weaker than capsaicin.

Results and discussion

Rat TRPV1 was heterologously expressed in CHO cells, using an inducible expression system. Interaction of evodiamine with TRPV1 was determined by competition of [^{3}H] RTX binding. Evodiamine inhibited [^{3}H] RTX binding with a K_i of 5.95 ± 0.87 μM (mean ± SEM, n = 3 experiments) (Fig. 2). Evodiamine was thus some 3-fold weaker than capsaicin for binding to rTRPV1 (capsaicin, K_i = 1.8 ± 0.3 μM).

The functional consequences of evodiamine binding to rTRPV1 were determined by uptake of $^{45}Ca^{2+}$. Evodiamine induced a

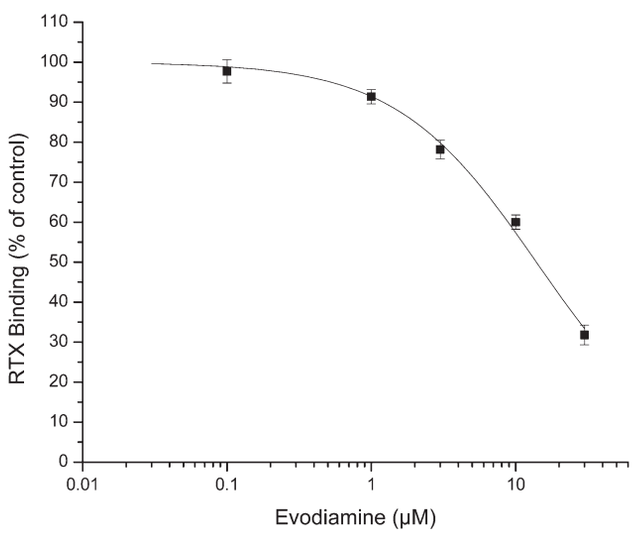

Fig. 2 Inhibition of [^{3}H] RTX binding to TRPV1 by evodiamine. Results shown are of a single, representative experiment, with all points determined in triplicate. Two additional experiments yielded similar results.

DOI: 10.1039/b404506h

similar level of $^{45}Ca^{2+}$ as did capsaicin, indicating that evodiamine functioned as a full agonist under these conditions (Fig. 3). The EC_{50} was 856 ± 43 (mean ± SEM, $n = 4$ experiments). For comparison, for capsaicin the $EC_{50} = 45 \pm 4$ nM, indicating that evodiamine was approximately 19-fold less potent under these conditions.

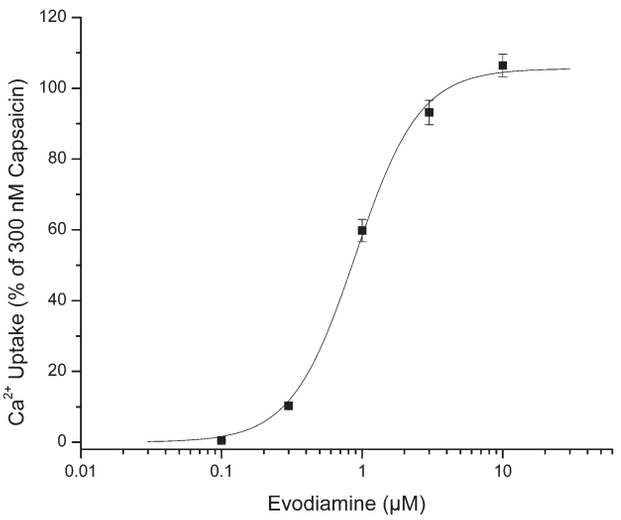

Fig. 3 Induction of $^{45}Ca^{2+}$ uptake by evodiamine in CHO-TRPV1 cells. Results shown are of a single, representative experiment, with all points determined in triplicate. Three additional experiments yielded similar results.

To probe the specificity of the action of evodiamine, we determined whether capsazepine, a competitive antagonist of capsaicin, could inhibit the $^{45}Ca^{2+}$ uptake induced by evodiamine. Capsazepine indeed blocked the action of evodiamine, shifting the dose response curve for the induction of $^{45}Ca^{2+}$ uptake to higher concentrations in a dose-dependent fashion [Fig. 4(a)]. Schild plot analysis indicated that the inhibition of evodiamine action by capsazepine was competitive [Fig. 4(b)], yielding an EC_{50} for evodiamine of 0.92 μM, a K_i for capsazepine of 0.67 μM, and a Hill coefficient of 2.33, indicating positive cooperativity.

Calcium imaging was used to assess the extent and kinetics of elevation of intracellular calcium in response to evodiamine treatment. Evodiamine (EVO) caused a rapid elevation in intracellular calcium; increasing doses caused increasing maximal levels of internal calcium but similar rates for achieving these plateau levels [Fig. 5(a)]. This pattern of response is similar to that for capsaicin (CAP) and contrasts with that of resiniferatoxin, for example, where increasing doses cause elevation in internal calcium but with similar maximal response.[7] The EC_{50} for evodiamine as determined by calcium imaging was 1.03 ± 0.21 μM (mean ± SEM, $n = 3$ experiments) [Fig. 5(b)]. This value agrees well with that determined by uptake of $^{45}Ca^{2+}$. To verify that the increase in intracellular calcium in response to evodiamine was dependent on TRPV1, we examined the response of control CHO cells, not expressing TRPV1. Negligible elevation of intracellular calcium levels by evodiamine was observed at up to 10 μM (data not shown).

In an initial step in understanding why evodiamine is able to bind to TRPV1 despite its apparent structural differences from other TRPV1 ligands, we superimposed evodiamine on capsaicin and ligands **1**–**3**,[8,9] which represent four structural classes of potent VR1 agonists, and assessed the similarity of the pharmacophore models derived from each pair of ligands. The superposition was performed using the Genetic Algorithm Similarity Program (GASP) (Tripos, Inc., St. Louis, MO). The best models for each pair of ligands are shown in Fig. 6. For each model the GASP identified four consistent pharmacophore elements: two lipophilic centers L1 and L2, two hydrogen bond acceptor groups A1 and A2, and a hydrogen bond donor group (D). The individual and average distances between the pharmacophore groups in these models are shown in Table 1. Interestingly, in A2 the distance between the N1

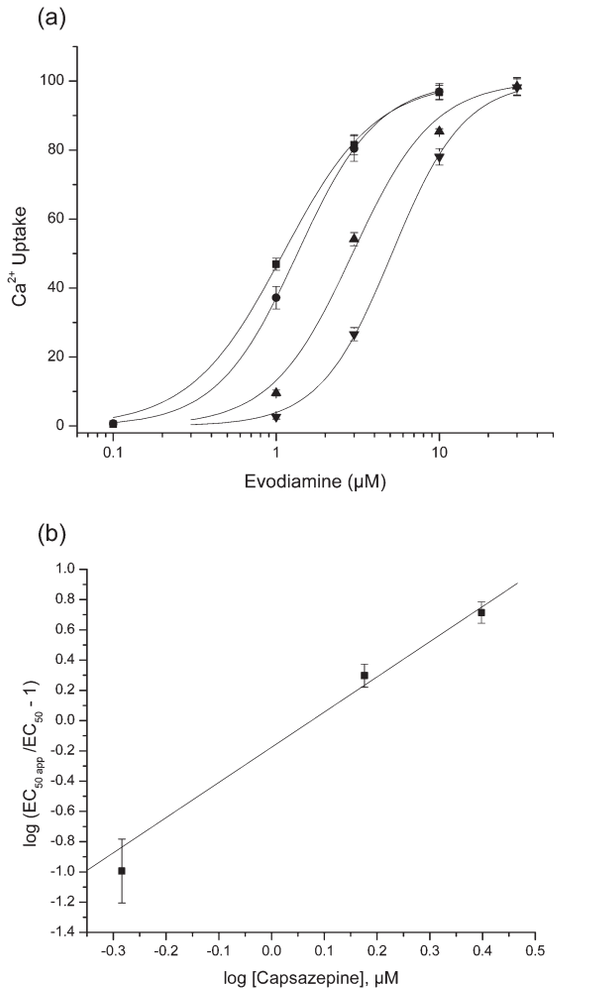

Fig. 4 Inhibition of evodiamine-induced $^{45}Ca^{2+}$ uptake by capsazepine. (a) Dose–response curves for induction of $^{45}Ca^{2+}$ uptake by evodiamine as a function of the indicated concentrations of the antagonist capsazepine (■, control; ●, 0.52 μM; ▲, 1.5 μM; ▼, 2.5 μM). Results shown are of a single, representative experiment, with all points determined in triplicate. Three additional experiments yielded similar results. (b) Schild plot. Points represent the average values from four experiments.

atom in evodiamine and the O1 atom or S1 atom in capsaicin and ligands **1**–**3** (Fig. 6) is relatively large (Table 1), which may indicate that the corresponding donor group in the protein has a relatively high tolerance to the position of the matching acceptor group. In general, all resulting models are very similar and all are consistent with the common features found in regions A, B, and C (Fig. 1) in the majority of the VR1 agonists,[10–12] which include two lipophilic centers in regions A and C and hydrogen bond donor and acceptor groups in region B.

To ensure that the identified active conformation of the evodiamine is relatively close to its global minimum,[13] we performed a conformational analysis of evodiamine. The energies of the resulting low energy conformations and of the active conformation identified by GASP were calculated using the PM3 Hamiltonian in MOPAC. It was found that evodiamine had three low energy conformations within 5 kcal mol^{-1} of the global minimum conformation D: two almost flat conformations A and B and a V-shaped conformation C (Fig. 7). The active conformation of evodiamine identified by GASP (34.94 kcal mol^{-1}) is only 1.52 kcal mol^{-1} higher than the lowest energy conformation D (33.42 kcal mol^{-1}) and is thus acceptable.[13]

We conclude that evodiamine is a full agonist at rat TRPV1 heterologously expressed in CHO cells. Its specificity of action is confirmed both by the lack of effect in the control CHO cells lacking TRPV1 and by its competitive mechanism relative to capsazepine, as evidenced by the Schild analysis. Its potency was 3-fold less than that of capsaicin in the binding assay and 19-fold less potent for calcium uptake. The difference in potency of evodiamine

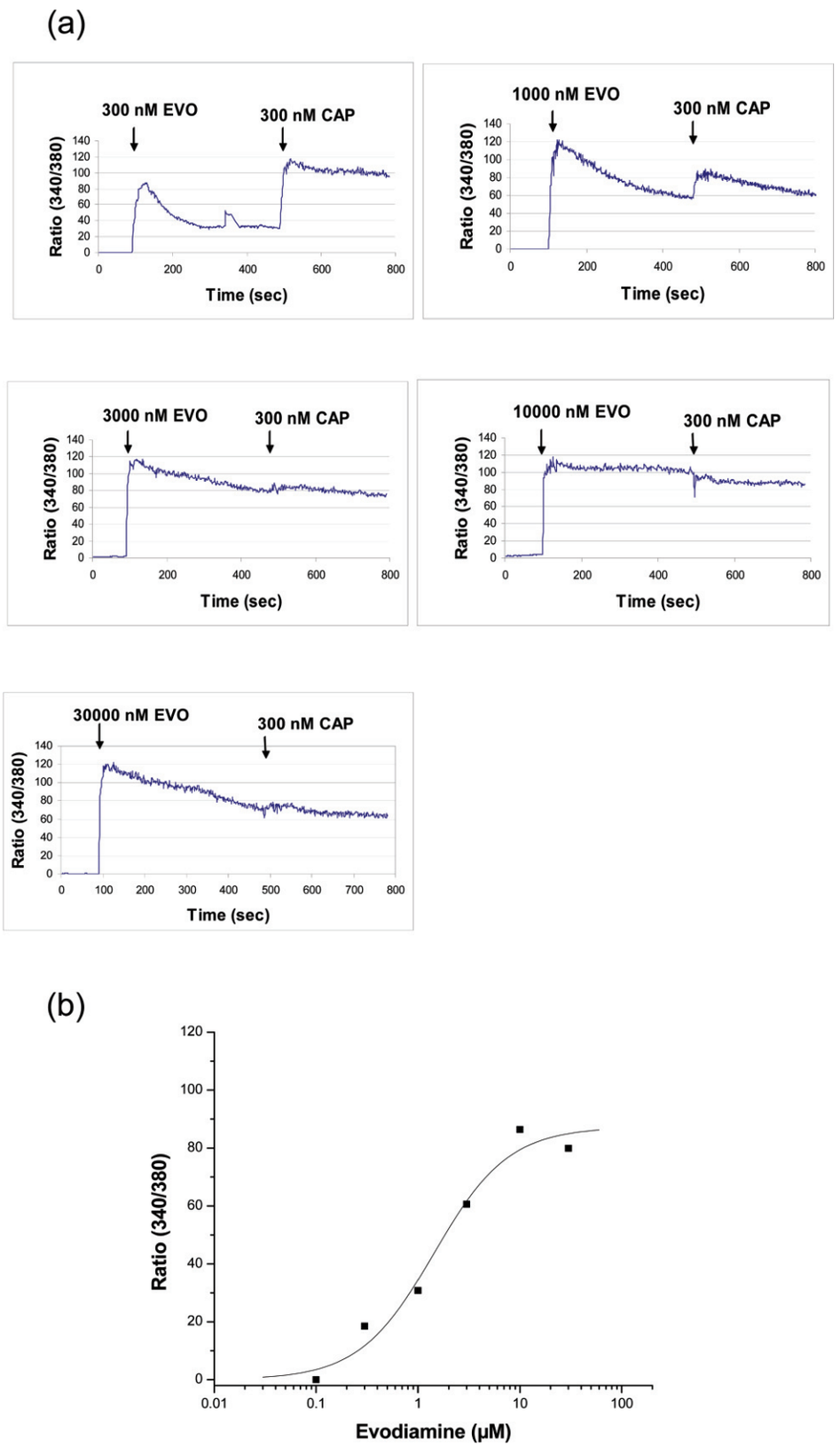

Fig. 5 Increase in intracellular calcium in response to evodiamine treatment. Response was detected as the change in the fluorescent ratio of the Fura-2 AM at 340 and 380 nm. (a) Representative time courses as a function of evodiamine concentration. The first arrow indicates the time of addition of evodiamine (EVO). The second arrow indicates the time of addition of 300 nM capsaicin (CAP). The curves represent the averaged data from 47 cells in a single experiment. Two additional experiments yielded similar results. (b) Dose–response curve for the increase in intracellular calcium as a function of evodiamine concentration. The maximal levels at different doses of evodiamine were expressed relative to the level induced by 300 nM capsaicin. Points represent a representative experiment. Two additional experiments yielded similar results.

between the two assays is not surprising, because differences in the structure–activity relations for different ligands in the two assays have been consistently observed previously, presumably reflecting multiple factors, including intrinsic differences between the total TRPV1 assayed in the binding assay and that subfraction present at the plasma membrane and involved in calcium uptake.[2]

Our values for evodiamine, moreover, are in general agreement with the findings of Kobayashi and co-workers,[4–6] who reported that evodiamine was 3-fold less active than capsaicin for inducing contractions of the guinea pig atrium and bronchi and was about 30-fold less potent for inducing nociception in the mouse paw licking assay.

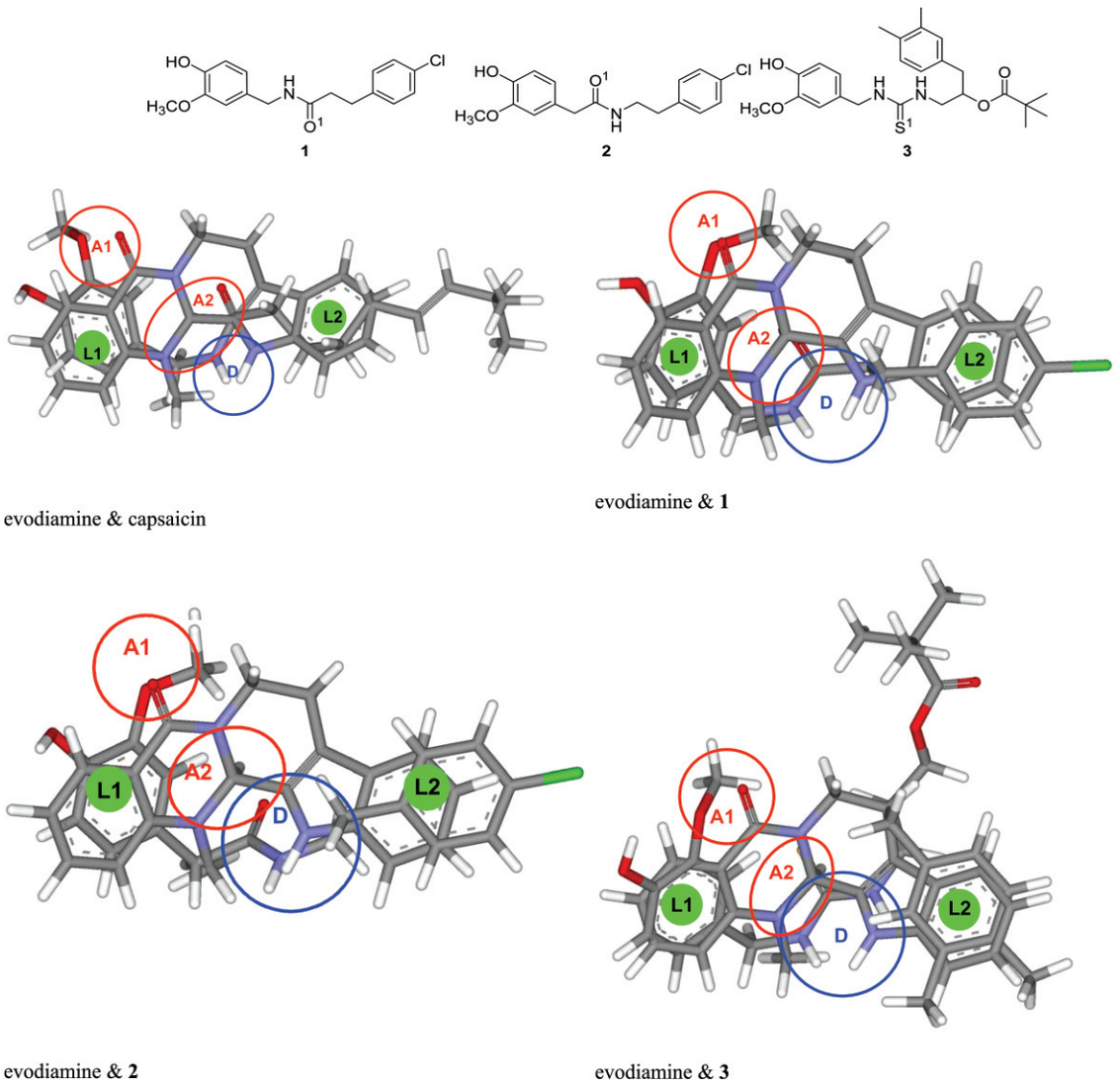

Fig. 6 Pharmacophore models built using superposition of evodiamine with capsaicin and ligands **1**–**3**. The hydrogen bond donor centroid is rendered by a blue circle, the hydrogen bond acceptor by a red circle, and the lipophilic centers (LC) 1 and 2 by green circles.

Table 1 Distances between the pharmacophore elements in the model of the VR1 receptor derived from the superposition of evodiamine with capsaicin and ligands **1**–**3**

	Distance/Å				
	Evodiamine & capsaicin	Evodiamine & **1**	Evodiamine & **2**	Evodiamine & **3**	Average
A1–L1	3.1	3.2	3.2	3.2	3.2
L1–D	4.5	4.3	4.8	4.3	4.5
D–L2	3.4	4.2	3.9	4.0	3.9
L2–A1	7.7	7.7	7.6	7.3	7.6
A1–D	5.5	5.2	5.5	5.2	5.4
L1–L2	7.5	8.0	8.2	7.7	7.9
A2–A1	4.0	4.0	4.3	4.1	4.1
A2–D	1.9	1.9	2.3	2.3	2.1
A2–L1	3.4	3.5	3.5	3.5	3.5
A2–L2	4.8	5.7	5.8	5.7	5.5
d_{A2}[a]	2.8	2.4	2.3	2.6	2.5

[a] Distance between the N1 nitrogen atom of evodiamine and the O1 oxygen of capsaicin, **1**, or **2** or the sulfur atom of **3**.

Evodiamine represents yet another example of the diverse structures that nature has designed for activation of TRPV1, a receptor for nociceptive stimuli. Because of its novel structure relative to other TRPV1 agonists, it affords a valuable lead structure for medicinal chemistry directed to this promising therapeutic target. In this regard, its limited conformational flexibility may be of particular value.

Materials and methods

Materials

Evodiamine was obtained from Pharm-Rx Chemical Corporation (Denville, NJ, USA). Resiniferatoxin (RTX) was obtained from Biomol (Plymouth Meeting, PA, USA). Capsaicin was from Sigma (St. Louis, MO, USA)

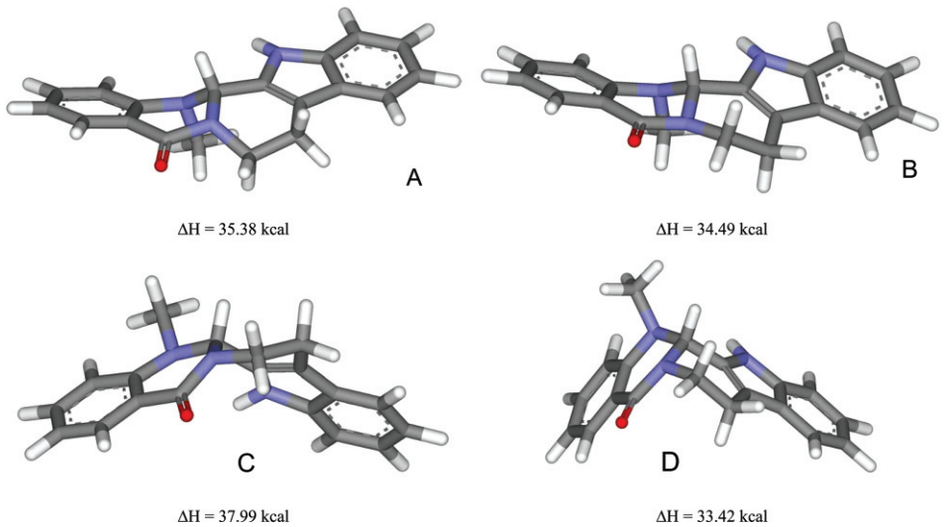

Fig. 7 Four low energy conformations of the evodiamine identified by CONFORT and their energies calculated using the MOPAC PM3 method.

Cell culture

The stably transfected CHO-VR1 cells were generously donated by James E. Krause and Daniel N. Cortright (Neurogen, Branford, CT). The CHO-VR1 cells were cultured in T-75 cm^2 flasks containing maintaining medium [Ham's F-12 supplemented with 10% FBS, 25 mM HEPES, pH 7.5, 250 μg ml^{-1} geneticin, and 1 μg ml^{-1} tetracycline (Calibochem, La Jolla, CA, USA)].

Harvesting CHO-VR1 cells for assay of ligand binding to TRPV1

After 48 h in the maintaining medium, at which time the cells had attained at least 90% confluency, they were washed twice with DPBS buffer (without Ca^{2+} and Mg^{2+}) and were cultured for an additional 2 d in an inducing medium (Ham's F-12 supplemented with 10% FBS, 25 mM HEPES, pH 7.5). The cells were then harvested in trypsin-EDTA, washed with DPBS, and the cell pellets stored as aliquots at −70 °C.

[^{3}H] RTX competition binding

The experiments were performed in borosilicate glass tubes containing the following components: Dulbecco's Phosphate-Buffered Saline (DPBS) supplemented with 0.25 mg ml^{-1} BSA, 100 nM cold RTX, [^{3}H] RTX, varying concentrations of a non-radioactive ligand, and a membrane fraction containing approximately 5×10^5 cells in a final volume of 350 μl. The mixture was incubated in a water bath for 60 min at 37 °C and then cooled on ice for 10 min. 100 μl of 2 mg ml^{-1} bovine glycoprotein fraction VI (AGP; ICN, Costa Mesa, CA, USA) was added to the tubes to reduce the non-specific binding by the RTX. The membranes were then pelleted by centrifugation for 15 min at maximum velocity in a Beckman Allegra 21R centrifuge to separate the membrane-bound RTX from the free ligand. The tips of the centrifuge tubes containing the pellets were cut off and the radioactivity in both the pellets and in aliquots of the supernatant were determined by liquid scintillation counting. The equilibrium binding parameters (K_i and cooperativity) were determined by fitting the Hill equation to the measured values with the aid of the MicroCal Origin program.

Ca^{2+} uptake

The CHO-VR1 cells were grown in 24-well plates to yield a density of 50–70% confluency. After 24 h, the maintaining medium was replaced with inducing medium to allow VR1 expression. Experiments were conducted 48 h after induction, and included the following materials: 400 μl of DMEM (Life Technologies, Rockville, MD, USA) supplemented with 0.25 mg ml^{-1} BSA, *ca.* 1 μCi ml^{-1} radioactive calcium (ICN, Costa Mesa, CA, USA), and increasing concentrations of the tested ligand. The plates were incubated in the water bath for 5 min at 37 °C. The plates were washed twice with DPBS (Life Technologies, Rockville, MD, USA), after which 400 μl of RIPA buffer (50 mM Tris-Cl, pH 7.4, 150 mM NaCl, 1% Triton X-100, 0.1% SDS, 1% sodium deoxycholate) was added to lyse the cells. Plates were placed on a shaker for approximately 30 min. Then, the radioactivity in 300 μl of the cell lysate from each well was determined by scintillation counting. Data were fitted to the Hill equation using the Quattro Pro and MicroCal Origin programs. Each point in each experiment was determined in triplicate. For the Schild plot analysis, the experiments were done in the presence of a vanilloid antagonist, capsazepine, at concentrations of 520 nM, 1.5 μM, and 2.5 μM.

Ca^{2+} imaging

CHO-VR1 cells were plated on 25 mm round glass coverslips in the maintaining medium. After 24 h, at which time the cells had attained approximately 30% confluency, the medium was replaced by the inducing medium supplemented with 1 mM sodium butyrate to induce VR1 expression. Experiments were conducted 24 h after induction. For Fura-2 AM loading, the cells were transferred to DPBS containing 0.25 mg ml^{-1} BSA and 10 μM Fura-2 AM (Molecular Probes, Eugene, OR, USA) for 1.5 h in the dark at room temperature. After up to 1.5 h, the loading solution was replaced with a maintaining medium and the cells were incubated for 1 h in the dark at room temperature before starting calcium measurements. Imaging was performed as described and the ratio of fluorescent intensity at 340 and 380 nm was determined.[2]

Molecular modeling methods

All calculations were performed using molecular modeling packages in Sybyl6.91 (Tripos, Inc., St. Louis, MO). All molecules were sketched and subjected to preliminary geometry optimization using the Tripos force field implemented in MAXIMIN2 minimizer. The conformational analysis of evodiamine was performed using CONFORT (Tripos, Inc., St. Louis, MO). The three low energy conformations of evodiamine within 5 kcal mol^{-1} of the global minimum A–C including the most stable conformation D were optimized using the MOPAC module and PM3 Hamiltonian. The parameters in the MOPAC were set to default values. The resulting set of conformations and their energies are shown in Fig. 7. Pairwise flexible superposition of evodiamine with capsaicin and ligands **1**–**3** [8,9] was performed using the GASP module in Sybyl6.91. The parameters in the GASP were set to default values. Both non-aromatic rings of evodiamine were allowed to flex. The best pharmacophore models were rendered using DS Modeling (Accelrys, Inc., San Diego, CA) and are shown

in Fig. 6. The distances between the pharmacophore elements are presented in Table 1.

References

1 D. Julius and A. L. Basbaum, *Nature*, 2001, **413**, 203–210.
2 A. Toth, P. M. Blumberg, Z. Chen and A. P. Kozikowski, *Mol. Pharmacol.*, 2004, **65**, 282–291.
3 G. Appendino, E. Munoz and B. L. Fiebich, *Expert Opin. Ther. Pat.*, 2003, **13**, 1825–1837.
4 Y. Kobayashi, Y. Nakano, K. Hoshikuma, Y. Yokoo and T. Kamiya, *Planta Med.*, 2000, **66**, 526–530.
5 Y. Kobayashi, K. Hoshikuma, Y. Nakano, Y. Yokoo and T. Kamiya, *Planta Med.*, 2001, **67**, 244–248.
6 Y. Kobayashi, *Planta Med.*, 2003, **69**, 425–428.
7 A. Szallasi, P. M. Blumberg, L. L. Annicelli, J. E. Krause and D. N. Cortright, *Mol. Pharmacol.*, 1999, **56**, 581–587.
8 C. S. Walpole, R. Wrigglesworth, S. Bevan, E. A. Campbell, A. Dray, I. F. James, K. J. Masdin, M. N. Perkins and J. Winter, *J. Med. Chem.*, 1993, **36**, 2381–2389.
9 J. Lee, J. Kim, S. Y. Kim, M. W. Chun, H. Cho, S. W. Hwang, U. Oh, Y. H. Park, V. E. Marquez, M. Beheshti, T. Szabo and P. M. Blumberg, *Bioorg. Med. Chem.*, 2001, **9**, 19–32.
10 C. S. Walpole, S. Bevan, G. Bovermann, J. J. Boelsterli, R. Breckenridge, J. W. Davies, G. A. Hughes, I. James, L. Oberer and J. Winter, *J. Med. Chem.*, 1994, **37**, 1942–1954.
11 H. Park, M. Park, J. Choi, S. Choi, J. Lee, Y. Suh, U. Oh, H. D. Kim, Y. H. Park, Y. S. Jeong, J. K. Choi and S. Jew, *Bioorg. Med. Chem. Lett.*, 2003, **13**, 197–200.
12 H. G. Park, M. K. Park, J. Y. Choi, S. H. Choi, J. Lee, B. S. Park, M. G. Kim, Y. G. Suh, H. Cho, U. Oh, H. D. Kim, Y. H. Park, H. J. Koh, K. M. Lim, J. H. Moh and S. S. Jew, *Bioorg Med. Chem. Lett.*, 2003, **13**, 601–604.
13 M. C. Nicklaus, S. Wang, J. S. Driscoll and G. W. Milne, *Bioorg. Med. Chem.*, 1995, **3**, 411–428.